ELSEVIER

Surface Science 391 (1997) L1178–L1182

surface science

Surface Science Letters

Oxygen desorption from α-Al_2O_3 (0001) supported Rh, Pt and Pd particles

E.S. Putna *, J.M. Vohs, R.J. Gorte

Department of Chemical Engineering, University of Pennsylvania, Philadelphia, PA 19104-6393, USA

Received 30 May 1997; accepted for publication 18 July 1997

Abstract

Temperature-programmed desorption (TPD) was used to study the interaction of oxygen with both large ($\sim$10 nm) and small (<2 nm) Rh, Pt and Pd particles supported on α-Al_2O_3(0001). The results of this study indicate that O_2 desorption from large particles of Rh, Pt and Pd is similar to that from low-index planes of the respective metal single crystals. Additionally, O_2 desorption from small Rh particles is similar to that from the close-packed planes of bulk Rh. In contrast, O_2 desorption from small particles of Pt and Pd occurs at a significantly higher temperature than that from the respective, low-index single crystal surfaces despite a much higher saturation oxygen coverage on the small particles. Possible explanations for the differences in O_2 desorption as a function of particle size for the various metals is discussed. © 1997 Elsevier Science B.V.

Keywords: Catalysis; Models of surface kinetics; Oxygen; Palladium; Platinum; Rhodium; Thermal desorption; Thermal desorption spectroscopy

Although most technologically interesting, precious-metal catalysts are composed of small metal particles supported on high-surface-area substrates, the majority of what we know about the nature of adsorbed species and the kinetics of surface reactions on metals has been determined from measurements on metal single crystals. This is due primarily to the ease of monitoring adsorption and desorption on these well-defined model systems. While numerous studies have been performed to relate the reactivity of bulk, single crystals to that of small supported-metal particles, mainly through studies of simple adsorbates such as CO [1–10], many important questions remain concerning the nature of adsorption and reaction on small-metal particles. For CO on precious metals, most changes in the desorption kinetics with particle size can be related to similar changes that occur with variations in exposed crystal plane [2–5,7,9]. With Pt, for example, very small particles ($\sim$2.0 nm) exhibit temperature-programmed-desorption (TPD) features similar to those observed for stepped single-crystal surfaces, while large particles ($\geq$10 nm) exhibit features similar to those for low-index planes such as the (111) surface. TPD studies of H_2 and NO suggest however, that simply equating the adsorptive properties of small particles to that of stepped surfaces and large particles to that of low-index surfaces is not appropriate [10–13].

Oxygen is an important molecule for which adsorption on small metal particles has not been extensively studied. Since, like CO, O_2 desorption

* Corresponding author. Fax: (+1) 215 573.2093; e-mail: vohs@eniac.seas.upenn.edu

PII S0039-6028(97)00611-0

temperatures are a function of the crystallographic orientation of precious-metal surfaces [14–18], O_2 desorption kinetics may also vary with the particle size of supported precious-metals. Metal particles smaller than approximately 2.5 nm [19–21] do not have the electronic band structure of a bulk metal. How this affects the interaction of oxygen with small metal particles is largely unknown.

In the present study, the adsorption of O_2 on small particles of Rh, Pt and Pd supported on an inert support, α-$Al_2O_3(0001)$, was examined using TPD. The use of a flat single-crystal support allowed readsorption and diffusion – effects which generally complicate the analysis of desorption measurements from high-surface-area materials – to be neglected [22]. The results of this study suggest that, although the interaction of oxygen with small metal particles is similar to that of bulk metals, particle size can affect the desorption kinetics possibly by changing the magnitude of adsorbate–adsorbate interactions.

The ultra-high vacuum (UHV), surface-analysis system used in this work was the same as that described in our previous studies [23]. The ion-pumped vacuum chamber had a base pressure of 3×10^{-10} torr and was equipped with a mass spectrometer and a cylindrical mirror analyzer for Auger electron spectroscopy (AES). The α-$Al_2O_3(0001)$ substrate was 3 mm in diameter and mounted on a Ta foil sample holder which could be resistively heated. A thermocouple was attached to the back surface of the α-$Al_2O_3(0001)$ crystal using a ceramic adhesive (Aremco 516). Rh, Pt and Pd were deposited using an evaporative metal source. The flux of metal atoms reaching the substrate was determined using a quartz-crystal, film-thickness monitor. Gases were exposed to the samples through directed, beam dosers. TPD measurements were carried out using a heating rate of 15 K/s.

After cleaning the α-$Al_2O_3(0001)$ crystal by ion bombardment at room temperature, it was annealed in 5×10^{-8} torr O_2 for 10 min at 1270 K and then oxidized in 5×10^{-8} torr O_2 for 30 min at 770 K. This produced a surface free from impurities as determined by AES. The metal of choice was then deposited onto the substrate, which was held at room temperature, followed by heating to 700 K. Our previous studies have shown that this procedure results in the formation of relatively uniform spherical particles for all three metals [8–13,23]. The average metal particle size was controlled by varying the amount of metal that was initially deposited. Average particle sizes were calculated from the known metal coverage and saturation CO coverages as determined by TPD. Table 1 lists the metal coverages and the resulting metal particle sizes of samples used in this study. In the dispersion measurements, it was assumed that the adsorption stoichiometry for CO was constant with particle size, even though small differences are known to exist [24]. Previous work comparing particle sizes calculated in this way with TEM measurements showed excellent agreement [13,23].

O_2 TPD data obtained from large and small particles of Rh, Pt and Pd, following a saturation exposure of O_2 at 300 K, are shown in Fig. 1–3. The ratio of the area of the O_2 desorption peak to that of the CO desorption peak (for a saturation CO coverage) is reported in Table 1 for each sample. As shown in Fig. 1, similar results were obtained for both the large (10 nm) and small (1.6 nm) Rh particles. For the large Rh particles, the onset of O_2 desorption occurs abruptly at 850 K, has a peak maximum centered at 915 K and has a broad tail that extends beyond 1300 K. For the small Rh particles, the main desorption

Table 1
Summary of the samples used in this study

Metal	Metal coverage (monolayers)	Particle size[a] (nm)	O_2:CO (ratio of TPD peak areas)[b]
Rh	0.25	1.6	1.0
	10.0	10.0	0.24
Pt	0.25	2.0	0.71
	10.0	8.3	0.26
Pd	0.25	1.6	0.60
	10.0	9.1	0.36

[a]Calculated from dispersion measurements using CO. The metal films were deposited onto the α-Al_2O_3 (0001) crystal at room temperature and heated briefly in vacuum to 700 K to form particles prior to CO adsorption.

[b]Ratio of the areas of the O_2 and CO TPD peaks normalized to the ratio for the 0.25×10^{15} Rh/cm^2 film.

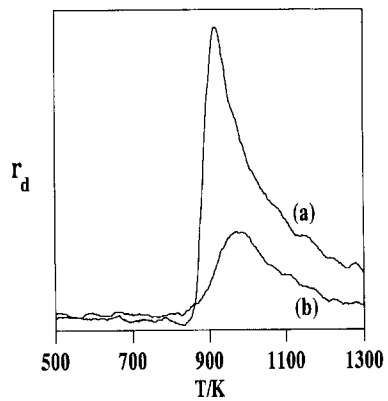

Fig. 1. O_2 TPD data for Rh particles: (a) 10 nm; (b) 1.6 nm, supported on α-Al_2O_3(0001). The data was obtained following a saturation dose of O_2 at 300 K.

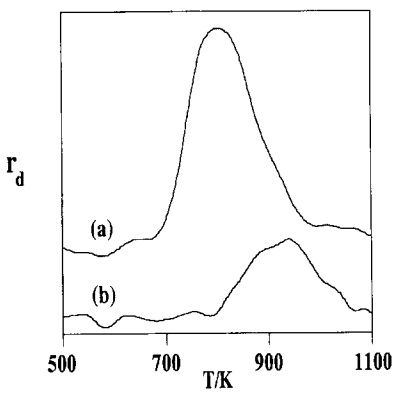

Fig. 2. O_2 TPD data for Pt particles: (a) 8.3 nm; (b) 2.0 nm, supported on α-Al_2O_3(0001). The data was obtained following a saturation dose of O_2 at 300 K.

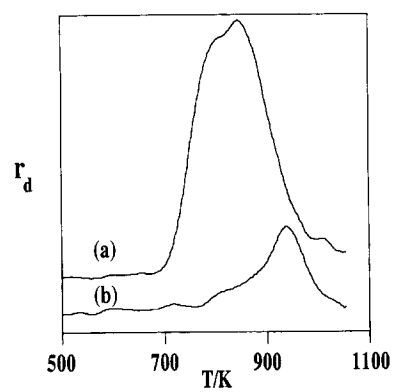

Fig. 3. O_2 TPD for Pd particles: (a) 9.1 nm; (b) 1.6 nm, supported on α-Al_2O_3(0001). The data was obtained following a saturation dose of O_2 at 300 K.

feature is somewhat less sharp and has a slightly higher peak temperature of 975 K; otherwise, the general desorption features are the same.

The O_2 TPD results for the Rh particles are similar to those reported previously for Rh particles 3–4 nm in size [25]. They are also similar to O_2 TPD curves obtained from Rh(111) [17,26] and Rh(100) [18]. The data from the single crystals also exhibit sharp O_2 desorption features near 900 K, with broad desorption tails which continue up to 1400 K. In all cases, the O_2 desorption peaks from the Rh surfaces do not follow classical second-order kinetics. Given that the TPD results for the various single crystal surfaces may differ in detail, but are largely similar, it is perhaps not surprising that particle-size effects on the O_2 desorption results are also minimal. There is some controversy over whether oxygen penetrates the near-surface region of Rh at temperatures below the onset of O_2 desorption [17,18]. If oxygen does go subsurface, the high-temperature shoulder could result from diffusion limitations, with the lower-temperature features corresponding to desorption of surface oxygen in the presence of the bulk oxide. Alternatively, the sharp desorption features could arise from repulsive interactions between adsorbed oxygen atoms. In either case, the adsorbed oxygen is apparently in a similar chemical environment on both the small Rh particles and the single-crystal surfaces.

The saturation coverage of oxygen on the small Rh particles was a factor of four higher than on the larger particles, as shown in Table 1. On Rh(111), the saturation coverage of adsorbed O_2 is 0.25 monolayers (ML) and results in a (2×2) LEED pattern [17]. Assuming that the saturation coverage of CO is 1 ML (i.e. the CO adsorption stoichiometry is one CO per exposed Rh atom), the data in Table 1 indicate that the saturation coverage of oxygen on the 10 nm Rh particles is also approximately 0.25 ML. This again suggests that the interaction of oxygen with the 10 nm Rh particles is similar to that of the low-index planes of Rh. It is interesting that the saturation oxygen coverage on the 1.6 nm Rh particles is roughly four times that on the 10 nm particles. This may result from the surfaces of the smaller particles being more disordered (i.e. contain more steps and defects) than

those of the larger Rh particles. Adsorbate repulsive interactions, which limit the saturation oxygen coverage to 0.25 ML on Rh(111), are likely to be less pronounced on the more disordered surfaces of the smaller Rh particles, thereby allowing for a higher oxygen coverage.

TPD results for small (2.0 nm) and large (8.3 nm) Pt particles obtained following a saturation dose of O_2 are displayed in Fig. 2. On the larger particles, the desorption peak is rather broad and centered near 800 K. In a separate set of experiments, it was found that, for subsaturation O_2 exposures, the O_2 desorption peak shifted to a higher temperature. Whilst one would expect an upward shift in the peak temperature with decreasing coverage for second-order kinetics, the observed shift was too large to be completely accounted for by this effect. For Pt single crystals, O_2 TPD curves are relatively independent of the crystallographic orientation of the surface [27–31] although one study has shown an additional low-temperature state at 650 K on Pt(100) [16]. The activation energy for O_2 desorption from Pt single crystal surfaces has been shown, however, to decrease with coverage, varying from 51 to 42 kcal/mol on Pt(111) [27]. This coverage dependence has been attributed to repulsive interactions between adsorbed oxygen atoms [27]. Since the O_2 desorption curves from the large Pt particles are similar to those reported for Pt(111), the variation in the O_2 peak temperature with coverage is most likely also due to repulsive interactions between the oxygen adatoms.

In contrast to Rh, the results for the large and small Pt particles were substantially different. Even though the saturation oxygen coverage was almost three times higher on the small Pt particles, the O_2 desorption temperature was 150 K higher on the small Pt particles relative to the large Pt particles. This suggests that the interaction of oxygen with the small particles is stronger than that on the large particles or that repulsive interactions are less important on the more disordered surfaces of the small particles. Unfortunately, we were unable to study the effect of the initial oxygen coverage on desorption from the small particles. If one assumes that repulsive interactions give rise to the shape of the desorption curves for the Rh particles, it is somewhat surprising that particle size affects O_2 desorption on Pt so much more strongly than on Rh.

Desorption curves for small (1.6 nm) and large (9.1 nm) Pd particles are shown in Fig. 3. On the large particles, there appears to be two, unresolved peaks near 800 and 875 K. When a sample with large Pd particles was cooled from 1000 to 300 K while being exposed to 10^{-7} torr O_2, a three-fold increase in the O_2 desorption peak area relative to that obtained following O_2 adsorption at 300 K was observed, with all of the additional desorption occurring between 600 and 700 K (see Fig. 4). Again, TPD curves obtained following subsaturation O_2 exposures gave desorption only at the higher temperatures. In contrast, the results for the smaller particles exhibit desorption in a much narrower temperature window, from 850 to 1000 K, with a peak maximum near 950 K.

Comparison of the O_2 desorption results from Pd, single-crystal surfaces with those obtained here for the large Pd particles reveals that the two are similar. On Pd(111), O_2 desorbs in a single peak between 800 and 900 K [14,32], while on Pd(100) and Pd(110), an additional O_2 peak centered at 700 K is observed [15,33–35]. Therefore, based on the single-crystal data, it appears that the more open non-close-packed surfaces give rise to higher oxygen coverages and additional low-temperature features. The fact that this does not lead to low-temperature desorption features in the case of the

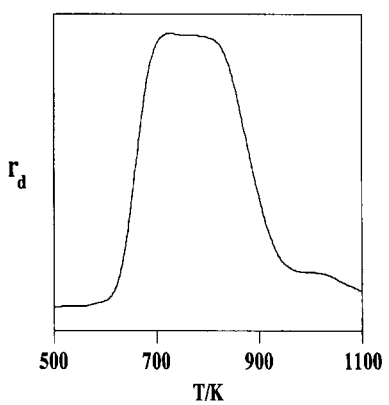

Fig. 4. O_2 TPD data for 9.1 nm Pd particles supported on α-Al_2O_3(0001). The sample was cooled from 1000 to 300 K in 10^{-7} torr of O_2 prior to the TPD experiment.

small particles in the present study is very surprising. As noted above, one would expect the small particles to behave more like non-close-packed or stepped single-crystal surfaces. In agreement with this, the relative coverage following a saturation exposure of O_2 is significantly higher on the small particles relative to the large particles. As was the case for Pt, it again appears that either oxygen binds more strongly to the small particles, possibly by going subsurface, or that repulsive interactions between oxygen adatoms are less important on the small particles.

Xu and Goodman have previously studied O_2 desorption from Pd particles formed following the deposition of 5 ML of Pd on a silica substrate [36]. Although this Pd coverage resulted in large Pd particles ($\sim$50 nm), the desorption results reported by Xu and Goodman are similar to what was observed for the small Pd particles in the present study. This is somewhat surprising but may result from the fact that the Pd particles appear to be oriented on the silica substrate.

Considering the results obtained from all three metals, it is clear that the interaction of oxygen with the large metal particles ($\sim$10 nm) is similar to that with the low-index planes of the respective bulk metals. However, for very small particles (1–2 nm), Rh is unique in that it maintains the complex shape of the desorption curves found on bulk Rh. The TPD curves for small particles of Pt and Pd are relatively featureless and do not exhibit the strong, downward shift in peak temperature one would expect for the high adsorbate coverages found on these surfaces.

Acknowledgements

This work was supported by the United States Department of Energy, Basic Energy Sciences, grants DE-FG03-85-13350 (RJG) and DE-FG02-96ER14682 (JMV). Some facilities were provided by the National Science Foundation through their materials research laboratory program (grant DMR 88-19885). Professor Vohs would also like to acknowledge Union Carbide Corporation for support provided through their Innovation Recognition Program.

References

[1] D.L. Doering, H. Poppa, J.T. Dickinson, J. Vac. Sci. Technol. 20 (1982) 827.
[2] D.L. Doering, H. Poppa, J.T. Dickinson, J. Vac. Sci. Technol. 18 (1981) 460.
[3] D.L. Doering, H. Poppa, J.T. Dickinson, J. Catal. 73 (1982) 104.
[4] S. Ichikawa, H. Poppa, M. Boudart, J. Catal. 91 (1985) 1.
[5] S. Ladas, H. Poppa, M. Boudart, Surf. Sci. 102 (1981) 151.
[6] D.W. Goodman, J. Vac. Sci. Technol. 20 (1982) 522.
[7] X. Xu, D.W. Goodman, Catal. Lett. 24 (1994) 31.
[8] E.I. Altman, R.J. Gorte, Surf. Sci. 192 (1988) 392.
[9] E.I. Altman, R.J. Gorte, Surf. Sci. 172 (1986) 71.
[10] H. Cordatos, T. Bunluesin, R.J. Gorte, Surf. Sci. 3 (1995) 219.
[11] E.I. Altman, R.J. Gorte, J. Catal. 110 (1988) 191.
[12] E.I. Altman, R.J. Gorte, J. Phys. Chem. 93 (1989) 1993.
[13] E.I. Altman, R.J. Gorte, J. Catal. 113 (1988) 185.
[14] D.L. Weissman, M.L. Shek, W.E. Spicer, Surf. Sci. 92 (1980) L59.
[15] M. Milun, P. Pervan, M. Vajic, K. Wandelt, Surf. Sci. 211/212 (1989) 887.
[16] G.N. Derry, P.N. Ross, Surf. Sci. 140 (1984) 165.
pp[17] P.A. Thiel, J.T. Yates, Jr., W.H. Weinberg, Surf. Sci. 82 (1979) 22.
[18] G.B. Fisher, S.J. Schmieg, J. Vac. Sci. Technol. A. 1 (1983) 1064.
[19] T.T.P. Cheung, Surf. Sci. 127 (1983) L129.
[20] E.H. Van Brockhoven, V. Ponec, Surf. Sci. 162 (1985) 731.
[21] R. Kubo, A. Kawabata, S. Kobayashi, Ann. Rev. Mater. Sci. 14 (1984) 49.
[22] R.J. Gorte, J. Catal. 75 (1982) 164.
[23] S. Roberts, R.J. Gorte, J. Phys. Chem. 93 (1990) 5337.
[24] J. Freel, J. Catal. 25 (1972) 149.
[25] E.S. Putna, J.M. Vohs, R.J. Gorte, J. Phys. Chem. 100 (1996) 17862.
[26] D.G. Castner, B.A. Sexton, G.A. Somorjai, Surf. Sci. 71 (1978) 519.
[27] C.T. Campbell, G. Ertl, H. Kuipers, J. Segner, Surf. Sci. 107 (1981) 220.
[28] J.L. Gland, V.N. Korchek, Surf. Sci. 75 (1978) 733.
[29] D.M. Collins, W.E. Spicer, Surf. Sci. 69 (1977) 85.
[30] L.D. Schmidt, Catal. Rev. 9 (1974) 115.
[31] R.W. McCabe, L.D. Schmidt, Surf. Sci. 60 (1976) 85.
[32] H. Conrad, G. Ertl, J. Kuppers, E.E. Latta, Surf. Sci. 65 (1977) 245.
[33] J.W. He, P.R. Norton, Surf. Sci. 204 (1988) 26.
[34] E.M. Stuve, R.J. Madix, C.R. Brundle, Surf. Sci. 146 (1984) 155.
[35] V.A. Bondzie, P. Kleban, D.J. Dwyer, Surf. Sci. 347 (1996) 319.
[36] X. Xu, D.W. Goodman, J. Phys. Chem. 97 (1993) 7711.